

FN⁺Cl Ions from Ionized F₂NCl: a Computational Investigation on the Structure and Reactivity toward H₂O

by Stefano Borocci, Nicoletta Bronzolino, and Felice Grandinetti*

Dipartimento di Scienze Ambientali and Istituto Nazionale di Fisica della Materia (INFM), Unità di Viterbo,
Università della Tuscia, L.go dell' Università, s.n.c., I-01100 Viterbo
(e-mail: fgrandi@unitus.it)

We have used various *ab initio* methods and basis sets to ascertain that the FN⁺Cl cation has a singlet ground state, ¹A', which is more stable than the triplet state ³A'' by *ca.* 30 kcal mol⁻¹. We have subsequently used the *Gaussian-3* (G3) theory to explore the potential-energy profile for the reaction between singlet FN⁺Cl and H₂O. The process commences by the effortless formation of a FN⁺Cl/H₂O complex, which, in principle, can undergo several alternative processes, including isomerization to *N*-protonated FN(Cl)OH, 1,2-elimination of HX (X = F or Cl), and 1,1-loss of H₂. However, the energy barriers of all these processes are invariably larger than the energy (+18.1 kcal mol⁻¹) required for the formation of FN⁺Cl/H₂O from FN⁺Cl and H₂O, thus suggesting that, under gas-phase thermal conditions, FN⁺Cl should be essentially unreactive toward H₂O. Comparing these theoretical findings with those concerning the reaction between FN⁺H, ClN⁺H, F₂N⁺, and H₂O, the reactivity order FN⁺H > F₂N⁺ > ClN⁺H > FN⁺Cl, was derived, which parallels the trend we recently found by G2MS calculations concerning the *Lewis* acidity of these ions. This suggests the conceivable occurrence of correlations between the reactivity and thermochemical properties of these simple halonitrenium ions.

1. Introduction. – Chloro(difluoro)amine, F₂NCl [1][2], has been proposed as an etchant for fabricating integrated circuits [3], and, more recently, as a fluorine-donor gas for preparing glass films of electronic materials with low dielectric constants [4]. During the industrial runs, gaseous mixtures containing F₂NCl and other volatile compounds are let into a vacuum chamber containing a substrate, and then activated by plasma methods. The role of F₂NCl is to provide the fluorine and chlorine atoms, which etch the solid surface or modify the composition of the deposited film. It is, however, conceivable that additional neutral and ionic species obtained from the plasma-induced fragmentation of F₂NCl affect the outcome of the industrial process. Particularly relevant are the F₂N⁺ and FN⁺Cl cations, which are the most-abundant ionic fragments obtained from the electron-impact ionization of F₂NCl [5]. It is, in fact, well known from experimental [6–8] and theoretical studies [9][10] that the F₂N⁺ ion, the dominant ionic fragment obtained from the ionization of NF₃ [11–16], plays an active role in the industrial etching and cleaning processes. Over the years, this has stimulated considerable experimental and theoretical interest in the chemistry of gaseous F₂N⁺ [17–34]. However, the structure, stability, and reactivity of FN⁺Cl are still very little explored.

In a recent theoretical investigation [35], we found that FN⁺Cl should be present in a singlet ground state (¹A') and behave as a *Lewis* acid that is much weaker than FN⁺H, ClN⁺H, and F₂N⁺. As a continuation of this study, we are reporting here more detailed theoretical evidence on the structure and stability of the singlet and triplet electronic

states of FN^+Cl , as well as the first theoretical insight into the reactivity of this cation. In particular, we have studied, at the *Gaussian-3* (G3) level of theory [36], the reaction between $^1\text{A}' \text{FN}^+\text{Cl}$ and H_2O , a nucleophile whose reactivity toward F_2N^+ , FN^+H , and ClN^+H in their singlet ground states, respectively, has been investigated in considerable detail [25][37][38], allowing comparison of the gas-phase reactivities of halonitrenium ions. The study of the reaction between FN^+Cl and H_2O is also of relevance for the chemistry of plasmas containing F_2NCl , since traces of moisture are usually unavoidable in industrial equipments used to perform etching and deposition processes.

2. Computational Methods. – Quantum-chemical calculations were performed with the *Unix* versions of GAUSSIAN 98 [39] and MOLPRO 2000.1 [40] sets of programs installed on a *Alphaserver 1200* and a *Compaq DS20E* machine.

The geometry of singlet and triplet FN^+Cl was optimized, with the 6-31G(d), 6-311G(d), 6-311G(2d), and 6-311G(2df) basis sets at the density functional level of theory [41], using the B3LYP functional [42–44], and at various *ab initio* levels of theory, including the second-order *Møller–Plesset* with inclusion of the inner electrons, MP2(full) [45]¹⁾, the *Quadratic Configuration Interaction* with single and double substitutions, QCISD [46], and the *Coupled Cluster* with inclusion of the contribution from single and double substitutions and of an estimate of connected triples, CCSD(T) [47][48].

The geometries of the various critical points (reactants, transition structures, intermediates, and products) involved in the reaction between singlet FNCI^+ and H_2O were fully optimized at the MP2(full)/6-31G(d) level, and the located structures were unambiguously characterized as true energy minima or first-order saddle points by calculating, at the same computational level, their analytical harmonic vibrational frequencies. Accurate total energies of all the investigated species were obtained at the MP2(full)/6-31G(d)-optimized geometries, using the *Gaussian-3* (G3) computational procedure by Pople and co-workers [36]. It consists of a sequence of well-defined *ab initio* calculations used to derive the total energy of a species according to an additivity scheme, the results of which are corrected by appending a small higher-level empirical term (HLC). The full details of the procedure are given in [36], and we simply report the expression used to calculate the G3 total energies (in hartree) at 0 K, *i.e.*, G3(0 K), of polyatomic, closed-shell species like those investigated in the present article:

$$\begin{aligned} \text{G3(0 K)} = & E[\text{MP4(fc)/6-31 + G(d)}] + E[\text{MP4(fc)/6-31G(2df,p)}] + E[\text{QCISD(T)/6-31G(d)}] \\ & - 2 \times E[\text{MP4(fc)/6-31G(d)}] + E[\text{MP2(full)/G3large}] - E[\text{MP2(fc)/6-31G(2df,p)}] \\ & - E[\text{MP2(fc)/6-31 + G(d)}] + E[\text{MP2(fc)/6-31G(d)}] - 0.006386n_{\text{val}} + \text{ZPE}. \end{aligned}$$

In the above equation, n_{val} is the number of valence-electron pairs, and *ZPE* is the zero-point energy calculated at the HF/6-31G(d) level and scaled by 0.8929 to take into account known deficiencies at this level [49]. The G3 total energies of the investigated species at 298.15 K, G3(298.15 K), were computed by adding to G3(0 K) a thermal correction calculated by standard statistical-mechanics formulae [50], using the scaled HF/6-31G(d) frequencies for the vibrations in the harmonic approximation, and the classical approximation for translation, $(3/2)RT$, and rotation (RT for linear species, $(3/2)RT$ for nonlinear species). The MP2(full)/6-31G(d) geometry optimizations and the G3 calculations were performed with the GAUSSIAN 98 program package. We used the 6-31G(d), 6-31 + G(d), and 6-31G(2df,p) basis-set standards in this program, whereas the G3large basis set, introduced in connection with the G3 theory, was downloaded from the website suggested in [36]. The 6-31G(d), 6-31 + G(d), and 6-31G(2df,p) basis sets use six *Cartesian* d-functions (6d), while the G3large basis set uses five ‘pure’ d-functions (5d). Both the 6-31G(2df,p) and G3large basis sets use a set of ‘pure’ 7f-functions.

¹⁾ The terms ‘full’ and ‘fc’ denote inclusion or no inclusion, respectively, of the inner electrons in the calculation of correlation energies.

3. Results and Discussion. – 3.1. *Structure and Stability of Singlet and Triplet FN⁺Cl.*

Before investigating the reaction with H₂O, we decided to get firm evidence on the electronic ground-state of FN⁺Cl by studying, at different computational levels and with various basis sets, the structures and stabilities of the corresponding singlet (¹A') and triplet (³A'') states. The results obtained are collected in *Table 1*.

Table 1. *Optimized Geometries* (bond lengths and angles in Å and °, resp.) *and Relative Stabilities* (Δ*E* in kcal mol^{−1}) of Singlet (¹A') and Triplet (³A'') FN⁺Cl

Calculation method	¹ A'			³ A''			Δ <i>E</i>
	N–F	N–Cl	F–N–Cl	N–F	N–Cl	F–N–Cl	
B3LYP/6-31G(d)	1.291	1.612	111.1	1.286	1.613	128.1	25.5
B3LYP/6-311G(d)	1.283	1.608	111.8	1.277	1.609	128.7	24.2
B3LYP/6-311G(2d)	1.285	1.605	111.5	1.280	1.602	128.6	24.9
B3LYP/6-311G(2df)	1.282	1.599	111.7	1.277	1.594	129.2	24.4
MP2(full)/6-31G(d)	1.308	1.573	110.8	1.289	1.572	129.7	34.2
MP2(full)/6-311G(d)	1.284	1.571	111.7	1.267	1.571	129.7	32.2
MP2(full)/6-311G(2d)	1.291	1.580	111.4	1.273	1.572	129.8	33.3
MP2(full)/6-311G(2df)	1.281	1.569	111.5	1.266	1.557	130.2	33.6
QCISD/6-31G(d)	1.309	1.606	110.8	1.299	1.614	128.4	27.1
QCISD/6-311G(d)	1.283	1.603	111.6	1.276	1.609	129.0	25.2
QCISD/6-311G(2d)	1.289	1.610	111.4	1.281	1.612	129.2	25.6
QCISD/6-311G(2df)	1.278	1.596	111.5	1.272	1.596	129.6	25.6
CCSD(T)/6-31G(d)	1.313	1.611	110.7	1.302	1.612	128.5	30.9
CCSD(T)/6-311G(d)	1.289	1.610	111.5	1.280	1.609	129.1	29.2
CCSD(T)/6-311G(2d)	1.296	1.618	111.2	1.285	1.612	129.2	29.8
CCSD(T)/6-311G(2df)	1.285	1.604	111.4	1.276	1.595	129.6	29.8

Generally speaking, R¹N⁺R² nitrenium ions, similar as their isoelectronic carbenes, possess a nonbonding electron pair and two nonbonding orbitals of similar energy [51 – 55]. Therefore, they can exist in both singlet and triplet states. In addition, in the singlet state, the electron pair resides in a nonbonding orbital centered on the N-atom and placed in the molecular plane. For this reason, the most-important structural difference between the singlet and triplet states of R¹N⁺R² concerns the R¹–N–R² bond angle, which turned out to be smaller for the singlet state. In the case of the parent system, H₂N⁺, it is well established, both experimentally [56][57] and theoretically [58–60], that the singlet state ¹A₁ gives rise to a bond angle of *ca.* 108°, and is less stable than the almost linear triplet ground state ³B₁ by *ca.* 30 kcal mol^{−1}. Replacing H-atom(s) with mono- or polyatomic substituents may substantially affect the relative stability of the two states, and, in fact, substituted nitrenium ions usually possess a singlet ground state. In particular, the results of the various *ab initio* calculations performed on the structure and stability of halonitrenium ions [17][19][21][22][29][34][61][62] have revealed that the XN⁺H species (X = F, Cl, Br, I) possess a singlet ground state, ¹A', which is more stable than the triplet state, ³A'' by *ca.* 8, 4, 6, and 7 kcal mol^{−1} for X = F, Cl, Br, and I, respectively. In addition, for the singlet-state ions, the X–N–H bond angle ranges from *ca.* 104° (X = F) to 109° (X = Cl), whereas the triplet-state ions have bond angles that range from *ca.* 125° (X = F) to 136° (X = I). For the X₂N⁺ ions, the calculated energy difference between the singlet ¹A₁ and the triplet ³B₁ states was invariably more pronounced than for XN⁺H, amounting to *ca.* 57, 20, 16, and 11 kcal

mol^{-1} for $X = \text{F}$, Cl , Br , and I , respectively. In addition, for the singlet-state ions, the $X-\text{N}-X$ bond angles range from *ca.* 108° ($X = \text{F}$) to 122° ($X = \text{I}$), whereas the triplet-state ions showed bond angles from *ca.* 125° ($X = \text{F}$) to 148° ($X = \text{I}$).

Concerning the $\text{N}-X$ bond distances of XN^+H and X_2N^+ , only minor differences were invariably found, when passing from the singlet to the triplet state [21]. As to FN^+Cl , we first note from *Table 1* that, at all levels considered, the singlet is more stable than the triplet state by *ca.* 30 kcal mol^{-1} . In addition, the structural differences between the two states are consistent with the available data concerning the XN^+H and X_2N^+ cations ($X = \text{F}$, Cl , Br , I). Thus, the $\text{F}-\text{N}-\text{Cl}$ bond angle (*ca.* 111°) of the singlet state is smaller than that of the triplet state (*ca.* 130°), whereas the $\text{N}-\text{F}$ and $\text{N}-\text{Cl}$ bond distances of the two states are quite similar (*Table 1*).

3.2. Reaction between FN^+Cl and H_2O . **3.2.1. Structure and Stability of Intermediates and Transition Structures.** Following the detailed investigation of the singlet and triplet electronic states of FN^+Cl , we decided to investigate the reaction between singlet-ground-state FN^+Cl and H_2O . The connectivities and the detailed MP2(full)/6-31G(d) geometries of the various intermediates involved in this process and of their interconnecting transition structures, respectively, are shown in *Figs. 1* and *2*, and in *Tables 2* and *3*.

The MP2 level should provide an adequate description of the structure of these species. Thus, it is well known that the properties of $\text{N}-\text{O}$ molecules, especially with halogen atoms present, are difficult to calculate [63]. However, investigations performed on the structure and stability of the nitrosyl halides FNO and ClNO [64][65] revealed that the MP2 theory gave rise to fairly accurate geometries, in accord with the CCSD method. In addition, it has been reported [66] that CCSD(T) wavefunctions, even in conjunction with the relatively small 6-31G(d) basis set, produces optimized geometries of the protonated FNO isomers, which were very similar to those found at the MP2 level of theory.

The adduct **1** (*Fig. 1*) formally arises from the direct association between FN^+Cl and H_2O . At the G3(0 K) level of theory, this process is exothermic ($-18.1 \text{ kcal mol}^{-1}$), which is consistent with our recent estimate of $-17.3 \text{ kcal mol}^{-1}$ [35] at the G2MS level of theory. Ion **1** can be also perceived as the *O*-protonated isomer of the hydroxylamine $\text{FN}(\text{Cl})\text{OH}$, and we note that, as expected, its computed $\text{N}-\text{O}$ bond distance of 1.791 \AA is significantly longer than in the unprotonated molecule (1.360 \AA). Isomer **2** formally arises from a '1,2 shift' of a H-atom from the O- to the N-atom of **1**; it can, therefore, be described as the *N*-protonated form of $\text{FN}(\text{Cl})\text{OH}$. At variance with **1**, the computed $\text{N}-\text{O}$ bond distance of **2**, 1.351 \AA , is slightly shorter than in $\text{FN}(\text{Cl})\text{OH}$. In addition, at the G3(0 K) level of theory, isomer **2** is predicted to be more stable than **1** by $10.6 \text{ kcal mol}^{-1}$. It is of interest to note here that, at the G3 level of theory, the *N*-protonated isomer of the hydroxylamines $X-\text{NH}-\text{OH}$ ($X = \text{F}$, Cl) was found to be more stable than the *O*-protonated isomer by 19.5 and $19.9 \text{ kcal mol}^{-1}$ for $X = \text{F}$ and Cl , respectively [38]. In addition, for hydroxylamine proper ($\text{H}_2\text{N}-\text{OH}$), the energy gap between the *O*- and the more-stable *N*-protonated isomers has been computed earlier as 25 kcal mol^{-1} at both the G1 [67] and G2 [68] levels of theory.

Upon searching for conceivable intermediates arising from the elimination of HX ($X = \text{F}$ or Cl) from **1** and **2**, we identified four distinct structures: **3**, **4**, **5**, and **6**. The optimized geometries of isomers **3** and **4** indicate the formation of loosely-bound

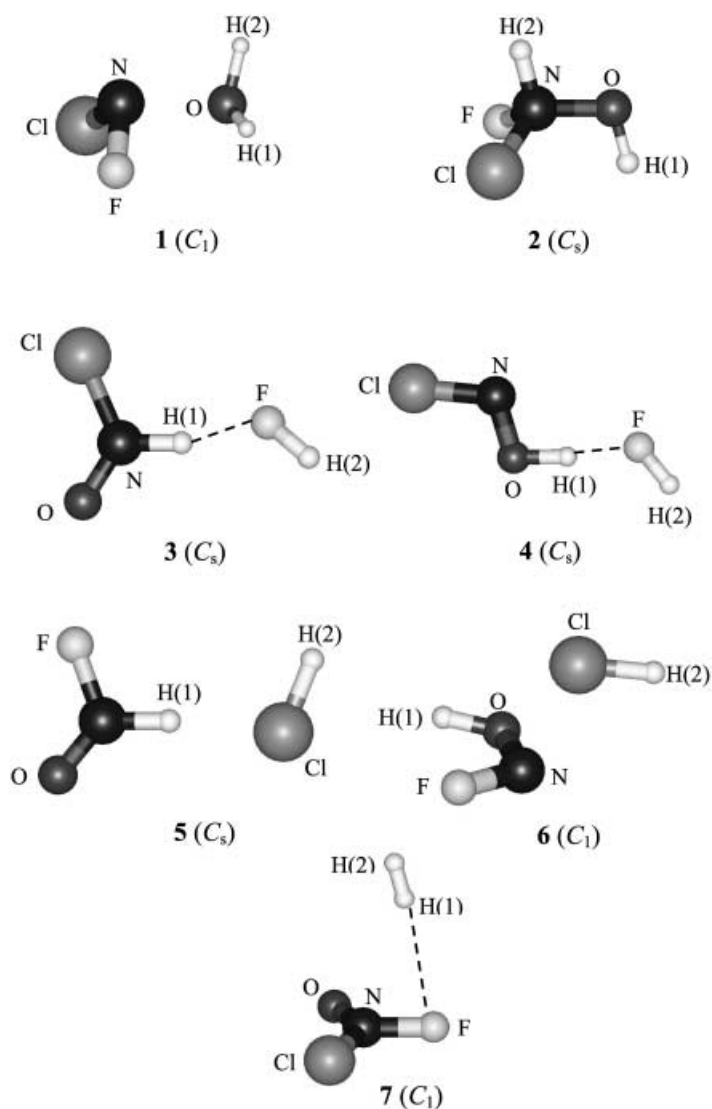


Fig. 1. Molecular connectivities of the intermediates **1**–**7** involved in the reaction between singlet FN^+Cl and H_2O . H-Bonds are indicated by dashed lines. The overall symmetries of the species are indicated in parentheses.

adducts between HF and the H-atom of $CIN^+(O)H$ or CIN^+OH . The computed F–H(1) bond of **3** (1.559 Å) is longer than in **4** (1.440 Å), and, consistently, at the G3(0 K) level of theory, the stability of the two adducts with respect to the dissociations into $CIN^+(O)H$ and HF or CIN^+OH and HF, respectively, was computed as 14.9 and 20.7 kcal mol^{−1}. Therefore, although the $CIN^+(O)H$ isomer is more stable than CIN^+OH by more than 11 kcal mol^{−1}, the latter interacts with HF more strongly than the former, and isomer **3** is more stable than **4** by only 5.6 kcal mol^{−1}.

Table 2. *MP2(full)/6-31G(d)-Optimized Geometries* (bond lengths d , bond and dihedral angles α and ϕ , resp.) of the Intermediates and Dissociation Products Involved in the Reaction between Singlet FN^+Cl and H_2O . For atom numbering, see Fig. 1.

Species		d [Å]		α [°]		ϕ [°]
1	N–O	1.791	N–O–H(1)	103.0	F–N–O–H(1)	31.4
	N–Cl	1.643	N–O–H(2)	102.1		
	N–F	1.361	F–N–Cl	107.5		
	O–H(1)	0.994	F–N–O	97.0		
	O–H(2)	0.993				
2	N–O	1.351	N–O–H(1)	106.1	H(1)–O–N–H(2)	179.2
	N–Cl	1.730	N–F–O	110.3		
	N–F	1.394	O–N–H(2)	104.8		
	O–H(1)	0.991				
	N–H(2)	1.039				
3	N–O	1.201	O–N–H(1)	121.7		
	N–Cl	1.669	Cl–N–O	123.6		
	N–H(1)	1.078	N–H(1)–F	167.0		
	F–H(1)	1.559	H(1)–F–H(2)	127.3		
	F–H(2)	0.948				
4	N–O	1.264	N–O–H(1)	105.8	Cl–N–O–H(1)	180.0
	N–Cl	1.628	Cl–N–O	111.8		
	O–H(1)	1.059	O–H(1)–F	173.3		
	F–H(1)	1.440	H(1)–F–H(2)	121.9		
	F–H(2)	0.950				
5	N–O	1.164	O–N–H(1)	128.8		
	N–F	1.349	F–N–O	120.5		
	N–H(1)	1.112	H(2)–Cl–H(1)	105.7		
	Cl–H(1)	1.289	N–H(1)–Cl	174.6		
	Cl–H(2)	1.924				
6	N–O	1.243	N–O–H(1)	113.7	F–N–O–H(1)	2.9
	N–Cl	2.735	F–N–O	109.3		
	N–F	1.323	N–Cl–H(2)	105.2		
	O–H(1)	1.017				
	Cl–H(2)	1.286				
7	Cl–O	3.289				
	N–O	1.170	N–O–H(1)	62.0		
	N–Cl	1.657	N–O–H(2)	69.7		
	N–F	1.354	F–N–O	119.9		
	O–H(1)	3.222	Cl–N–O	128.9		
	O–H(2)	3.740				
	F–H(1)	2.783				
	N–H(1)	2.866				
	N–O	1.308	H–N–O	111.3		
	N–Cl	1.709	Cl–N–O	115.8		
$\text{ClN}^+(\text{O})\text{H}$	N–H	1.037				
	N–O	1.295	Cl–N–O	11.9		
	N–Cl	1.684	H–O–N	112.2		
ClN^+OH	O–H	1.099			Cl–N–O–H	0.0
	N–O	1.279	F–N–O	116.1		
	N–F	1.325	F–N–H	110.0		
$\text{FN}^+(\text{O})\text{H}$	N–H	1.042				
	N–O	1.262	F–N–O	105.8		
	N–F	1.311	H–O–N	110.7		
FN^+OH	O–H	1.001			F–N–O–H	0.0
	N–O	1.298	Cl–N–O	116.2		
	N–F	1.336	Cl–N–F	111.9		
$\text{ClN}^+(\text{O})\text{F}$	N–Cl	1.739				
	N–F	1.308	F–N–Cl	110.8		
	N–Cl	1.572				
H_2O	O–H	0.969	H–O–H	104.0		
HF	H–F	0.934				
HCl	H–Cl	1.280				
H_2	H–H	0.738				

Similar to **3** and **4**, the isomers **5** and **6** are loosely bound adducts between HCl and the two ions $\text{FN}^+(\text{O})\text{H}$ or FN^+OH . The former species is more stable than the latter by *ca.* 10 kcal mol⁻¹, but the interaction energy of the former with HCl, 27 kcal mol⁻¹, is larger than for FN^+OH (17 kcal mol⁻¹). Thus, isomer **5** is more stable than **6** by *ca.* 20 kcal mol⁻¹. This significant difference in the stability of the two ions is mirrored in their computed structures. Particularly, in **5**, the ligation of HCl to $\text{FN}^+(\text{O})\text{H}$ occurs through the H-atom, whereas in **6** the Cl-atom of HCl interacts with the N–O bond of FN^+OH , although the N...Cl distance (2.735 Å) is shorter than the O...Cl distance (3.289 Å).

Isomers **4** and **6** can be perceived as the *F*- and the *Cl*-protonated forms of the hydroxylamine $\text{FN}(\text{Cl})\text{OH}$, and it is of interest to note that the former is more stable by more than 40 kcal mol⁻¹. As a matter of fact, **4** is the most stable among the various isomeric structures of protonated $\text{FN}(\text{Cl})\text{OH}$, thus suggesting that the F-atom is the thermochemically favored protonation site.

Species **7** is an intermediate involved in the unimolecular loss of H₂ from isomer **1**. The optimized geometry of this ion indicates the formation of a loosely bound adduct arising from the weak interaction of H₂ with the F-atom of the $\text{CIN}^+(\text{O})\text{F}$ cation. The F...H(1) distance is as large as 2.783 Å, and the interaction energy between the two moieties is lower than 0.5 kcal mol⁻¹.

The conversion of **1** into **2** occurs through the transition structure **TS1** (Fig. 2). The single imaginary frequency of this three-centers species, computed as 1774.0i cm⁻¹, refers to the in-plane motion of the H-atom, which shifts from the O- to the N-atom. The activation energy of this process was computed as 38.2 kcal mol⁻¹ from the G3(0 K) energy difference between **TS1** and **1**. In the transition structure **TS1**, the N–O bond distance, computed as 1.621 Å, is slightly shortened with respect to the intermediate **1** (1.791 Å), and the migrating H-atom lies in between the O- and N-atoms.

The extrusion of HF from the intermediate **1**, under formation of the intermediate **4**, occurs through the four-center transition structure **TS2**. The single imaginary frequency of this ion, computed as 1472.2i cm⁻¹, refers to the in-plane motion of the H-atom, which shifts from the O- to the F-atom. The O...H(2) and N–F bonds of **TS2**, computed as 1.287 and 1.646 Å, respectively, are significantly longer with respect to **1**, and, overall, an appreciable structural rearrangement is required to overcome the activation barrier, computed as 22.9 kcal mol⁻¹ at the G3(0 K) level of theory. Similarly, the extrusion of HCl from **1**, with formation of the intermediate **6**, occurs through the four-center transition structure **TS3**. The single imaginary frequency of this ion, computed as 1458.0 cm⁻¹, refers to the in-plane motion of the H-atom, which shifts from the O- to the Cl-atom. The O...H(2) and N–Cl bond distances, computed as 1.384 and 1.880 Å, respectively, are significantly longer with respect to **1**, and the activation barrier is computed to be as large as 28.1 kcal mol⁻¹ at the G3(0 K) level of theory. Also, the energy of **TS3** is higher than that of **TS2** by almost 5 kcal mol⁻¹.

The loss of H₂ from the O-atom of **1** occurs through the transition structure **TS4**, whose single imaginary frequency of 1878.3i cm⁻¹ refers to the symmetric stretching of the two O–H bonds, which appear to be appreciably longer relative to **1**. The N–O bond length of **TS4**, 1.285 Å, is also smaller than in **1** by *ca.* 0.5 Å, and, overall, a significant structural rearrangement is observed when passing from **1** to **TS4**.

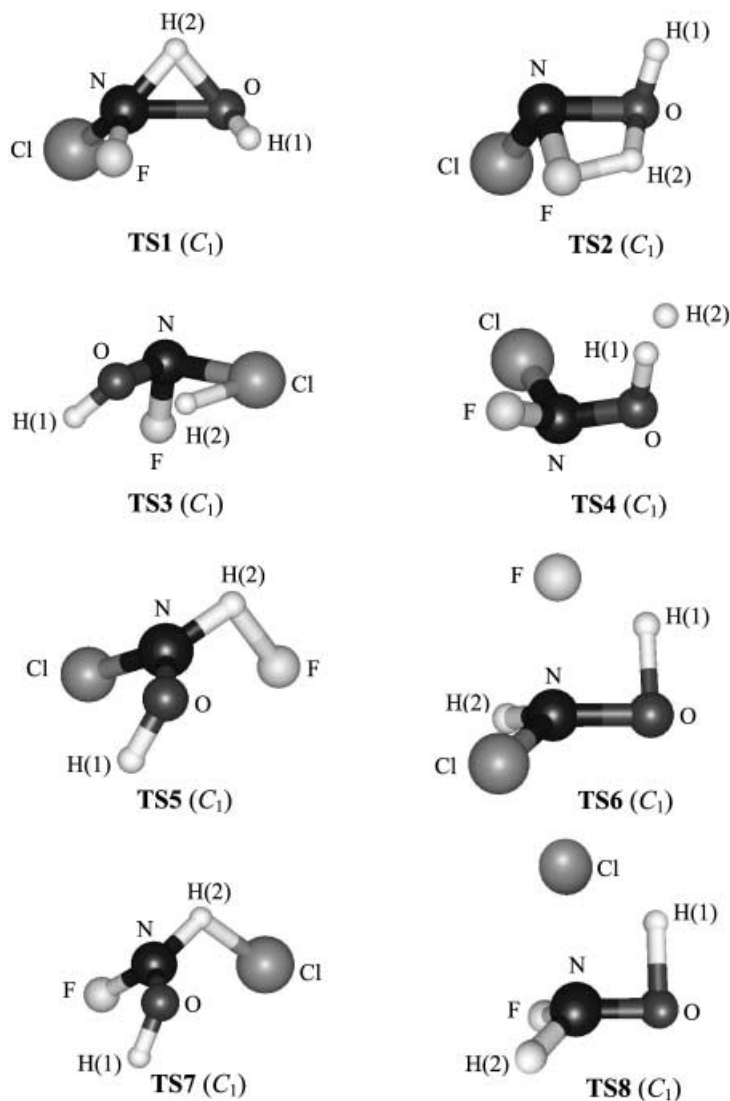


Fig. 2. Molecular connectivities of the transition structures **TS1**–**TS8** involved in the reaction between singlet FN^+Cl and H_2O . The overall symmetries of the species are indicated in parentheses.

Consistently, at the G3(0 K) level of theory, the energy difference between the two structures is computed to be as large as $79.3 \text{ kcal mol}^{-1}$, and **TS4** is the highest-energy species among the presently investigated ones.

Next, we investigated the mechanism of the loss of HF or HCl from the intermediate **2**. Both of these processes may, in principle, occur by two distinct paths, *i.e.*, either 1,1-abstraction of HX from the N-atom ($X=F$ or Cl) under eventual formation of **4** or **6**, or 1,2-elimination of HX under eventual formation of the

Table 3. *MP2(full)/6-31G(d)-Optimized Geometries* (bond lengths d , bond and dihedral angles α and ϕ , resp.) of the Transition Structures Involved in the Reaction between Singlet FN^+Cl and H_2O . For atom numbering, see Fig. 2.

Species		d [Å]		α [°]		ϕ [°]
TS1	N–O	1.621	O–N–H(2)	50.9	H(1)–O–N–F	8.2
	N–Cl	1.663	N–O–H(1)	103.8		
	N–F	1.358	N–O–H(2)	48.9		
	O–H(1)	1.001	F–N–O	105.5		
	O–H(2)	1.276	Cl–N–F	111.9		
	N–H(2)	1.240	Cl–N–H(2)	131.1		
TS2	N–O	1.498	N–O–H(1)	103.6	H(1)–O–N–Cl	143.5
	N–Cl	1.628	N–O–H(2)	79.6		
	N–F	1.646	F–N–O	84.8		
	O–H(1)	0.998	Cl–N–F	106.2		
	O–H(2)	1.287	Cl–N–O	107.4		
	F–H(2)	1.178	N–F–H(2)	76.7		
TS3	N–O	1.480	N–O–H(1)	107.4	H(1)–O–N–F	28.8
	N–Cl	1.880	F–N–O	103.3	O–N–Cl–H(2)	
	N–F	1.362	Cl–N–O	90.5		7.8
	O–H(1)	0.998	N–Cl–H(2)	69.5		
	O–H(2)	1.384				
	Cl–H(2)	1.493				
TS4	N–O	1.285	N–O–H(1)	113.5	H(1)–O–N–F	37.6
	N–Cl	1.686	N–O–H(2)	114.6		
	N–F	1.364	F–N–O	110.6		
	O–H(1)	1.197	Cl–N–O	117.4		
	O–H(2)	1.510				
	H(1)–H(2)	1.042				
TS5	N–O	1.285	N–O–H(1)	112.2	H(1)–O–N–Cl	18.6
	N–Cl	1.654	Cl–N–O	119.6		
	N–F	1.806	O–N–H(2)	116.9		
	O–H(1)	1.002	N–H(2)–F	96.6		
	F–H(2)	1.254				
	N–H(2)	1.164				
TS6	N–O	1.273	N–O–H(1)	88.7	H(1)–O–N–Cl	130.8
	N–Cl	1.644	F–N–O	87.4		
	N–F	1.782	Cl–N–F	118.4		
	O–H(1)	1.189	Cl–N–O	119.4		
	F–H(1)	1.328	Cl–N–H(2)	114.8		
	N–H(2)	1.041				
TS7	N–O	1.276	N–O–H(1)	111.2	H(1)–O–N–F	19.0
	N–Cl	2.248	F–N–O	113.6		
	N–F	1.341	Cl–H(2)–N	107.1		
	O–H(1)	1.005				
	Cl–H(2)	1.581				
	N–H(2)	1.199				
TS8	N–O	1.244	F–N–O	116.9	H(1)–N–O–H(2)	128.3
	N–Cl	2.074	Cl–N–O	94.5		
	N–F	1.376	N–O–H(1)	90.2		
	O–H(1)	1.309				
	Cl–H(1)	1.628				
	N–H(2)	1.046				

intermediates **3** or **5**. Indeed, our calculations showed all four transition structures **TS4**, **TS5**, **TS6**, and **TS7**.

The 1,1-elimination of HF from **2** occurs through the three-center transition structure **TS5**, whose single imaginary frequency of $1621.3i\text{ cm}^{-1}$ refers to the in-plane motion of the H-atom from the O- to the F-atom. The activation barrier of this process was computed as $32.9\text{ kcal mol}^{-1}$ from the G3(0 K) energy difference between **TS5** and **2**. The four-center transition structure **TS6**, whose single imaginary frequency of $2112.8i\text{ cm}^{-1}$ refers to the in-plane motion of the H-atom from the O- to the F-atom, is higher in energy than **TS5** by 6.7 kcal mol^{-1} . Therefore, the loss of HF from **2** is predicted to occur practically exclusively by a 1,1- rather than a 1,2-abstraction process. Similarly, the loss of HCl from **2** is predicted to occur by a 1,1- rather than a 1,2-mechanism. Indeed, at the G3(0 K) level of theory, the transition structure for the 1,1-loss, *i.e.*, **TS7**, is more stable than that for the 1,2-loss, **TS8**, by 4.6 kcal mol^{-1} . Also, the absolute values of 43.4 and $48.0\text{ kcal mol}^{-1}$ predicted for the activation barriers of these two processes are larger than the activation barriers for the corresponding processes involving HF. As for **TS5** and **TS6**, the single imaginary frequencies of the three- and four-center transition structures **TS7** and **TS8**, respectively, computed as $1555.5i$ and $2447.7i\text{ cm}^{-1}$, refer to the in-plane motion of the H-atom from the O- to the Cl-atom.

3.2.2. Competitive Reaction Pathways. The absolute and relative energies, at the G3(0 K) level of theory, of the various intermediates, transition structures, and dissociation products involved in the reaction between singlet FN^+Cl and H_2O , reported in Table 4, have been used to generate the diagram shown in Fig. 3.

The first important conclusion we draw from the potential-energy profile shown in Fig. 3 is that, under gas-phase thermal conditions, singlet FN^+Cl is predicted to be essentially unreactive toward H_2O . In fact, generally speaking, according to the double-well-potential model for gas-phase ion/molecule reactions [69], the collision between a cation A^+ and a neutral molecule B may eventually result in the efficient formation of ionic and neutral product(s) only when the energy gained in the usually unhindered association of the two fragments under formation of an $[\text{A}-\text{B}]^+$ complex is higher than the various activation barriers the latter species has to overcome to undergo formation of a given reaction product. According to Fig. 3, the energy ($18.1\text{ kcal mol}^{-1}$) gained in the association between FN^+Cl and H_2O under formation of **1** is appreciably lower than the activation barriers for the hydrolysis of this ion into FN^+OH and HCl ($28.1\text{ kcal mol}^{-1}$) and into $\text{FN}^+(\text{Cl})\text{O}$ and H_2 ($79.3\text{ kcal mol}^{-1}$), as well as for the interconversion with isomer **2** ($38.2\text{ kcal mol}^{-1}$). However, the transformation of **1** into ClN^+OH and HF involves an activation barrier of only $22.9\text{ kcal mol}^{-1}$, which is not far from the exothermic heat of reaction upon formation of **1** from FN^+Cl and H_2O , assuming an uncertainty of *ca.* 2 kcal mol^{-1} in the computed values. However, if one includes the thermal and entropy contributions at 298.15 K, the free energy change for the association between FN^+Cl and H_2O is 9.1 kcal mol^{-1} , which is significantly lower than the free energy barrier for the decomposition of **1** into ClN^+OH and HF ($23.7\text{ kcal mol}^{-1}$). Therefore, the only reaction channel probably accessible from the collision between FN^+Cl and H_2O , *i.e.*, the elimination of HF, should be observed only at very low temperatures and with a very low efficiency.

3.3. Reactivity of FN^+H , ClN^+H , F_2N^+ , and FN^+Cl toward H_2O . As already mentioned in the Introduction, the reactions of the halonitrenium ions FN^+H , ClN^+H ,

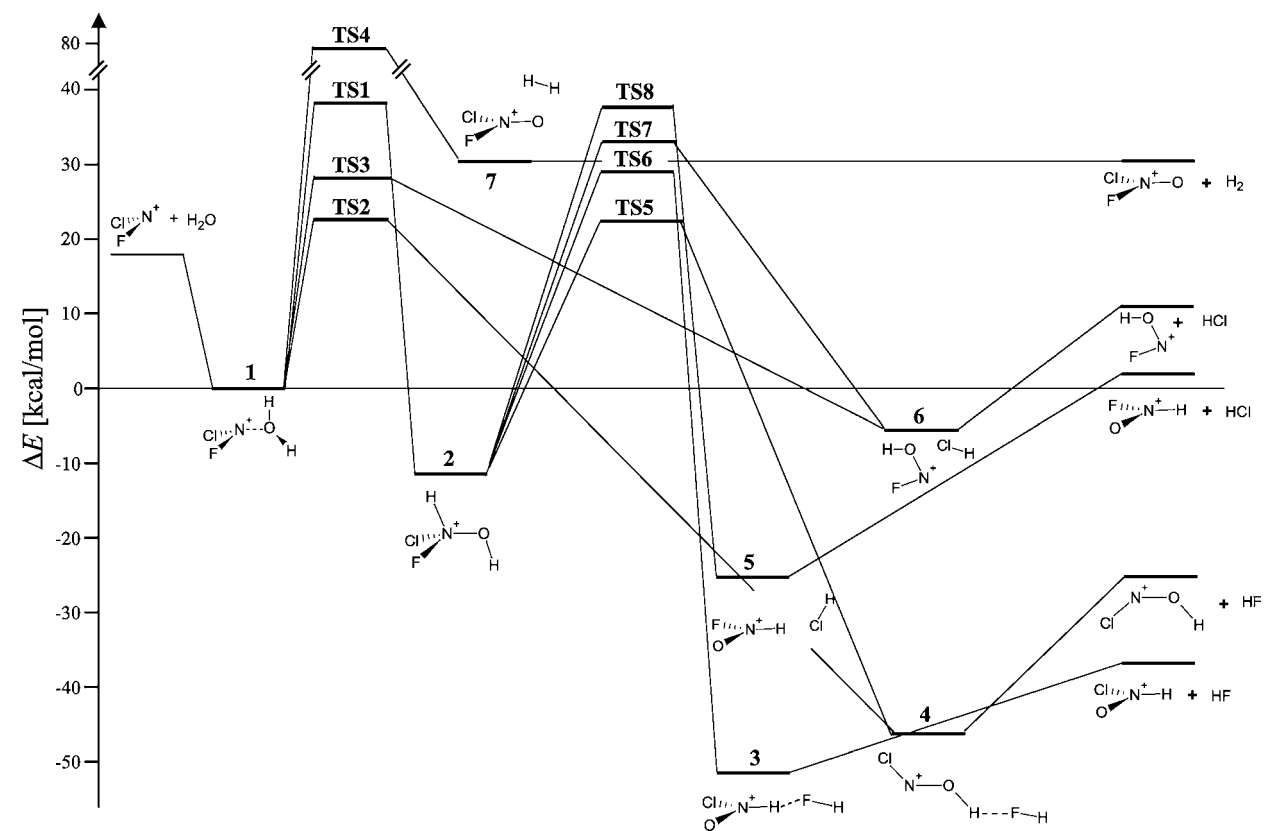


Fig. 3. $G3(0\text{ K})$ Relative energies (in kcal mol⁻¹) of the intermediates, transition structures, and dissociation products involved in the reaction between singlet FN^+Cl and H_2O

Table 4. Absolute and Relative Energies (in atomic units and kcal mol⁻¹, resp.) and MP2/6-31G(d) Total Entropies (*S*, in cal mol⁻¹ K⁻¹) of the Species Involved in the Reaction between Singlet FN⁺Cl and H₂O

Species	G3(0 K)	G3(298.15 K)	<i>S</i> (298.15 K)	Δ <i>E</i> (G3(0 K))
1	– 690.455048	– 690.449844	73.2	0.0
2	– 690.471931	– 690.467841	68.1	– 10.6
3	– 690.536847	– 690.530877	79.0	– 51.3
4	– 690.527841	– 690.521912	77.8	– 45.7
5	– 690.495152	– 690.489229	80.1	– 25.2
6	– 690.463342	– 690.457177	79.5	– 5.2
7	– 690.406661	– 690.399460	84.7	– 30.4
TS1	– 690.394229	– 690.389822	69.3	38.2
TS2	– 690.418554	– 690.414401	68.3	22.9
TS3	– 690.410293	– 690.405853	69.4	28.1
TS4	– 690.328658	– 690.324168	69.3	79.3
TS5	– 690.419512	– 690.415220	69.2	22.3
TS6	– 690.408797	– 690.404685	68.7	29.0
TS7	– 690.402785	– 690.398135	71.0	32.8
TS8	– 690.395500	– 690.391144	69.5	37.4
FN ⁺ Cl	– 614.042884	– 614.039806	61.4	
CIN ⁺ OH	– 590.093022	– 590.089848	61.6	
FN ⁺ OH	– 229.797009	– 229.793967	59.1	
CIN ⁺ (O)F	– 689.238596	– 689.235003	66.1	
CIN ⁺ (O)H	– 590.111319	– 590.108163	61.6	
FN ⁺ (O)H	– 229.812879	– 229.809857	59.0	
H ₂	– 1.167616	– 1.165255	31.1	
H ₂ O	– 76.383370	– 76.380536	45.1	
HF	– 100.401760	– 100.399399	41.5	
HCl	– 460.639176	– 460.636815	44.6	

and F₂N⁺ and H₂O have been investigated in considerable detail [25][37][38], and the lowest-energy portions of the corresponding potential-energy profiles are reported in Fig. 4.

On the basis of the diagrams in Figs. 3 and 4, we came to the conclusion that FN⁺Cl should be less reactive towards H₂O than FN⁺H, CIN⁺H, and F₂N⁺.

Like the reaction between FN⁺Cl and H₂O, the above reactions invariably start with the formation of XN⁺H/H₂O (X = F, Cl) or F₂N⁺/H₂O complexes, which may, in turn, undergo two lowest-energy processes: 1,2-elimination of HX or isomerization to the *N*-protonated hydroxylamine XN(H)OH (X = F, Cl) or F₂NOH. For FN⁺H (see Fig. 4, *a*) the energy gained in the formation of the FN⁺H/H₂O complex, 52.1 kcal mol⁻¹, is large enough to allow both isomerization to FN⁺(H₂)OH or formation of HN⁺OH by 1,2-elimination of HF. However, the energy difference of the transition structures involved in these two processes, *ca.* 8 kcal mol⁻¹, is large enough to support the expectation that the reaction between FN⁺H and H₂O should occur efficiently, leading to nearly exclusive elimination of HF. When passing to F₂N⁺ (see Fig. 4, *b*), we still expect exclusive 1,2-elimination of HF under formation of FN⁺OH, since the ‘isomerization’ of the F₂N⁺/H₂O complex to FN⁺OH/HF is the only process whose energy barrier, computed as 27 kcal mol⁻¹, is lower than the association energy between F₂N⁺ and H₂O (36 kcal mol⁻¹). These two values are, however, close enough to suggest that, compared with FN⁺H, the process should occur less efficiently. As a matter of fact, we have

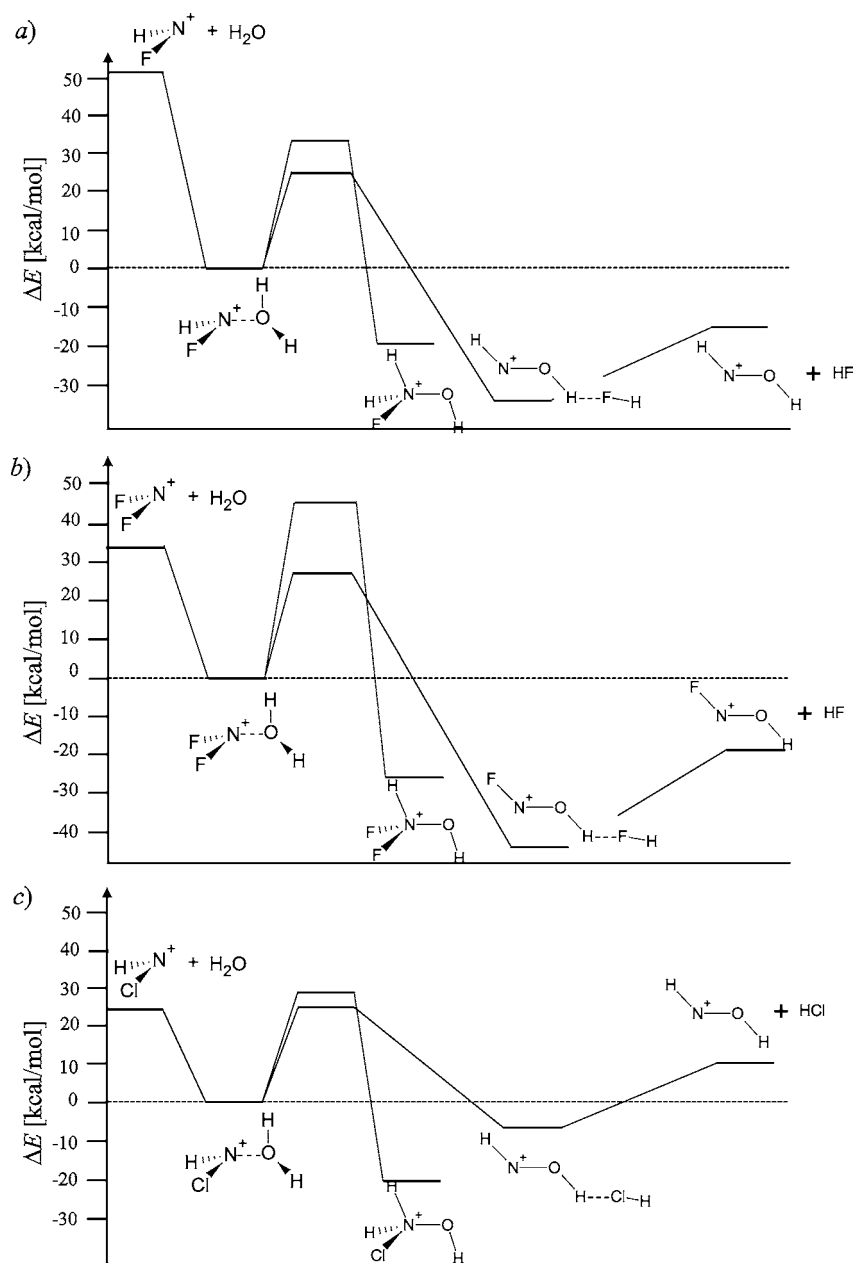


Fig. 4. $G3(0\text{ K})$ Relative energies (in kcal mol^{-1}) of the lowest-energy intermediates, transition structures, and dissociation products involved in the reaction between H_2O and a) singlet FN^+H , b) singlet F_2N^+ , and c) ClN^+H

observed experimentally [25] that the reaction between F_2N^+ and H_2O leads to the exclusive, but scarcely efficient, elimination of HF. Concerning ClN^+H (Fig. 4,c), the energy of formation of the $\text{ClN}^+\text{H}/\text{H}_2\text{O}$ complex from ClN^+H and H_2O , 24 kcal mol^{-1} , is comparable not only with the energy barrier for the isomerization to the $\text{ClN}^+(\text{H}_2)\text{OH}$ intermediate (28 kcal mol^{-1}), but also with the energy barrier for the formation of the $\text{HN}^+\text{OH}/\text{HCl}$ complex (24 kcal mol^{-1}). Taking into account an uncertainty of *ca.* 2 kcal mol^{-1} in these G3-computed values, the three values are nearly the same, and the ClN^+H cation should react with H_2O even less efficiently than F_2N^+ .

Concerning FN^+Cl , we have already discussed in the previous paragraph that the energy barriers of all the unimolecular processes involving the $\text{FN}^+\text{Cl}/\text{H}_2\text{O}$ complex are higher than the energy liberated upon ligation between FN^+Cl and H_2O , and this ion is expected to be basically unreactive toward H_2O . Therefore, in conclusion, the results of our calculations support the reactivity order $\text{FN}^+\text{H} > \text{F}_2\text{N}^+ > \text{ClN}^+\text{H} > \text{FN}^+\text{Cl}$ towards H_2O . Interestingly we have recently found by G2MS calculations [35] that the Lewis acidity of the above ions – quantified as the dissociation enthalpy at 298.15 K of the $\text{XN}^+\text{H}/\text{L}$, $\text{X}_2\text{N}^+/\text{L}$ ($\text{X} = \text{F}, \text{Cl}$), and $\text{FN}^+\text{Cl}/\text{L}$ adducts ($\text{L} = \text{HF}, \text{HCl}, \text{H}_2\text{O}, \text{H}_2\text{S}, \text{NH}_3, \text{PH}_3$) – follow a quite similar trend. This suggests the conceivable occurrence of correlations between the reactivity of the simplest halonitrenium ions and their thermochemical properties.

4. Conclusions. – Our calculations clearly indicate that the gaseous FN^+Cl cation has a singlet ground state $^1\text{A}'$, which is more stable than the triplet $^3\text{A}''$ state by *ca.* 30 kcal mol^{-1} . Concerning the reaction between $^1\text{A}' \text{ FN}^+\text{Cl}$ and H_2O , our calculations indicate that this cation is significantly less reactive than other fluoro- and chloronitrenium ions such as FN^+H , ClN^+H , and F_2N^+ . This raises the question on the actual role of FN^+Cl in the chemistry of plasmas containing F_2NCl , whose detailed investigation clearly deserves further experimental and theoretical work.

The authors wish to thank the Italian Ministero dell' Istruzione, dell' Università e della Ricerca (MIUR) and the Consiglio Nazionale delle Ricerche (CNR) for financial support.

REFERENCES

- [1] H. H. Sisler, in 'Encyclopedia of Inorganic Chemistry', Ed. R. B. King, John Wiley & Sons, N. Y., 1994, Vol. 5, p. 2545.
- [2] J. V. Gilbert, R. A. Conklin, R. D. Wilson, K. O. Christe, *J. Fluorine Chem.* **1990**, *48*, 361.
- [3] J. A. Barkanic, US Patent 5275692, 1994.
- [4] M. L. O'Neill, B. K. Peterson, J. L. Vincent, R. N. Vritis, EP Patent 1260606, 2002.
- [5] NIST Mass Spec Data Center, 'Mass Spectra', in NIST Chemistry WebBook, NIST Standard Reference Database Number 69, Eds. P. J. Linstrom, W. G. Mallard, March 2003, National Institute of Standards and Technology, Gaithersburg MD, 20899 (<http://webbook.nist.gov>).
- [6] T. W. Little, F. S. Ohuchi, *Surf. Sci.* **2000**, *445*, 235.
- [7] J. G. Langan, S. E. Beck, B. S. Felker, S. W. Rynders, *J. Appl. Phys.* **1996**, *79*, 3886.
- [8] M. Konuma, E. Bauser, *J. Appl. Phys.* **1993**, *74*, 62.
- [9] A. Endou, T. W. Little, A. Yamada, K. Teraishi, M. Kubo, S. S. C. Ammal, A. Miyamoto, M. Kitajima, F. S. Ohuchi, *Surf. Sci.* **2000**, *445*, 243.
- [10] A. Jenichen, *J. Phys. Chem.* **1996**, *100*, 9820.
- [11] P. D. Haaland, C. Q. Jiao, A. Garscadden, *Chem. Phys. Lett.* **2001**, *340*, 479.
- [12] V. Tarnovsky, A. Levin, K. Becker, R. Masner, M. Schmidt, *Int. J. Mass Spectrom. Ion Processes* **1994**, *133*, 175.

- [13] R. Rüede, H. Troxler, C. Beglinger, M. Jungen, *Chem. Phys. Lett.* **1993**, 203, 477.
- [14] D. P. Seccombe, G. K. Jarvis, B. O. Fisher, R. P. Tuckett, *Chem. Phys.* **1999**, 250, 335.
- [15] H. Baumgärtel, H.-W. Jochims, E. Rühl, H. Bock, R. Dammel, J. Minkwitz, R. Nass, *Inorg. Chem.* **1989**, 28, 943.
- [16] T. M. Miller, J. F. Friedman, A. E. Stevens Miller, J. F. Paulson, *J. Phys. Chem.* **1994**, 98, 6144.
- [17] J. F. Harrison, C. W. Eakers, *J. Am. Chem. Soc.* **1973**, 95, 3467.
- [18] J. J. Fisher, T. B. McMahon, *J. Am. Chem. Soc.* **1988**, 110, 7599.
- [19] K. A. Peterson, R. C. Mayrhofer, E. L. Sibert III, R. C. Woods, *J. Chem. Phys.* **1991**, 94, 414.
- [20] F. Grandinetti, J. Hrušák, D. Schröder, S. Karrass, H. Schwarz, *J. Am. Chem. Soc.* **1992**, 114, 2806.
- [21] A. Gobbi, G. Frenking, *Bull. Chem. Soc. Jpn.* **1993**, 66, 3153.
- [22] Z.-L. Cai, *Chem. Phys. Lett.* **1993**, 202, 70.
- [23] F. Cacace, F. Grandinetti, F. Pepi, *Angew. Chem., Int. Ed.* **1994**, 33, 123.
- [24] M. Aschi, F. Cacace, F. Grandinetti, F. Pepi, *J. Phys. Chem.* **1994**, 98, 2713.
- [25] M. Aschi, F. Grandinetti, F. Pepi, *Int. J. Mass Spectrom. Ion Processes* **1994**, 130, 117.
- [26] F. Cacace, F. Grandinetti, F. Pepi, *J. Chem. Soc., Chem. Commun.* **1994**, 2173.
- [27] F. Cacace, F. Grandinetti, F. Pepi, *J. Phys. Chem.* **1994**, 98, 8009.
- [28] F. Cacace, F. Grandinetti, F. Pepi, *Inorg. Chem.* **1995**, 34, 1325.
- [29] M. E. Jacox, W. E. Thompson, *J. Chem. Phys.* **1995**, 102, 6.
- [30] K. Hiraoka, M. Nasu, S. Fujimaki, S. Yamabe, *J. Phys. Chem.* **1995**, 99, 15822.
- [31] F. Grandinetti, F. Pepi, A. Ricci, *Chem.–Eur. J.* **1996**, 2, 495.
- [32] M. Aschi, F. Grandinetti, V. Vinciguerra, *Chem.–Eur. J.* **1998**, 4, 2366.
- [33] A. Ricca, *Chem. Phys. Lett.* **1998**, 294, 454.
- [34] F. Grandinetti, V. Vinciguerra, *Int. J. Mass Spectrom.* **2002**, 216, 285.
- [35] N. Bronzolino, F. Grandinetti, *THEOCHEM* **2003**, 635, 221.
- [36] L. A. Curtiss, K. Raghavachari, P. C. Redfern, V. Rassolov, J. A. Pople, *J. Chem. Phys.* **1998**, 109, 7764.
- [37] M. Marquez, F. Mari, C. A. Gonzalez, *J. Phys. Chem. A* **1999**, 103, 6191.
- [38] P. Facchini, F. Grandinetti, *J. Comput. Chem.* **2003**, 24, 547.
- [39] M. J. Frish, G. W. Trucks, H. B. Schlegel, G. E. Scuseria, M. A. Robb, J. R. Cheeseman, V. G. Zakrzewski, J. A. Montgomery, R. E. Stratman, J. C. Burant, S. Dapprich, J. M. Millam, A. D. Daniels, K. N. Kudin, M. C. Strain, O. Farkas, J. Tomasi, V. Barone, M. Cossi, R. Cammi, B. Mennucci, C. Pomelli, C. Adamo, S. Clifford, J. Ochterski, G. A. Petersson, P. Y. Ayala, Q. Cui, K. Morokuma, D. K. Malick, A. D. Rabuck, K. Raghavachari, J. B. Foresman, J. Cioslowski, J. V. Ortiz, B. B. Stefanov, G. Liu, A. Liashenko, P. Piskorz, I. Komaromi, R. Gomperts, R. L. Martin, D. J. Fox, T. Keith, M. A. Al-Laham, C. Y. Peng, A. Nanayakkara, C. Gonzalez, M. Challacombe, P. M. W. Gill, B. G. Johnson, W. Chen, M. W. Wong, J. L. Andres, M. Head-Gordon, E. S. Replogle, J. A. Pople, GAUSSIAN 98 (Revision A.6), Gaussian, Inc., Pittsburgh PA, 1998.
- [40] H.-J. Werner, P. J. Knowles, R. D. Amos, A. Bernhadsson, A. Berning, P. Celani, D. L. Cooper, M. J. O. Deegan, A. J. Dobbyn, F. Eckert, C. Hampel, G. Hetzer, T. Korona, R. Lindh, A. W. Lloyd, S. J. McNicholas, F. R. Manby, W. Meyer, M. E. Mura, A. Nicklass, P. Palmieri, R. Pitzer, G. Rauhut, M. Schatz, H. Stoll, A. J. Stone, R. Tarroni, T. Thorsteinsson, MOLPRO (<http://www.molpro.net>).
- [41] W. Koch, M. C. Holthausen, 'A Chemist's Guide to Density Functional Theory', Wiley-VCH, Weinheim, 2000.
- [42] A. D. Becke, *J. Chem. Phys.* **1993**, 98, 5648.
- [43] C. Lee, W. Yang, R. G. Parr, *Phys. Rev. B: Condens. Matter* **1988**, 37, 785.
- [44] P. J. Stephens, F. J. Devlin, C. F. Chabalowski, M. J. Frish, *J. Phys. Chem.* **1994**, 98, 11623.
- [45] C. Møller, M. S. Plesset, *Phys. Rev.* **1934**, 46, 618.
- [46] J. A. Pople, M. Head-Gordon, K. Raghavachari, *J. Chem. Phys.* **1987**, 87, 5968.
- [47] K. Raghavachari, G. W. Trucks, J. A. Pople, M. Head-Gordon, *Chem. Phys. Lett.* **1989**, 157, 479.
- [48] C. Hampel, K. Peterson, H.-J. Werner, *Chem. Phys. Lett.* **1992**, 190, 1.
- [49] A. P. Scott, L. Radom, *J. Phys. Chem.* **1996**, 100, 16502.
- [50] D. McQuarrie, 'Statistical Mechanics'; Harper & Row, N. Y., 1976.
- [51] P. G. Gassman, *Acc. Chem. Res.* **1970**, 3, 26.
- [52] R. A. Abramovitch, R. Jeyaraman, 'Azides and Nitrenes: Reactivity and Utility', Ed. E. F. V. Scriven, Academic Press, Orlando, 1984, p. 297.
- [53] T. P. Simonova, V. D. Nefedov, M. A. Toropova, N. F. Kirillov, *Russ. Chem. Rev.* **1992**, 61, 584.
- [54] R. A. McClelland, *Tetrahedron* **1996**, 52, 6823.
- [55] D. E. Falvey, *Mol. Supramol. Photochem.* **2000**, 6, 249.

- [56] S. T. Gibson, J. P. Greene, J. Berkowitz, *J. Chem. Phys.* **1985**, 83, 4319.
- [57] Y. Song, X.-M. Qian, K.-C. Lau, C. Y. Ng, J. Liu, W. Chen, *J. Chem. Phys.* **2001**, 115, 2582.
- [58] J. C. Stephens, Y. Yamaguchi, C. D. Sherill, H. F. Schaeffer, III, *J. Phys. Chem. A* **1998**, 102, 3999; J. C. Stephens, Y. Yamaguchi, C. D. Sherill, H. F. Schaeffer, III, *THEOCHEM* **1999**, 461/462, 41.
- [59] C. J. Cramer, F. J. Dulles, J. W. Storer, S. E. Worthington, *Chem. Phys. Lett.* **1994**, 218, 387.
- [60] D. A. Dixon, D. Feller, K. A. Peterson, *J. Chem. Phys.* **2001**, 115, 2576.
- [61] R. K. Milburn, C. F. Rodriguez, A. C. Hopkinson, *J. Phys. Chem. B* **1997**, 101, 1837.
- [62] C. Gonzalez, A. Restrepo-Cossio, M. Márquez, K. B. Wiberg, M. De Rosa, *J. Phys. Chem. A* **1998**, 102, 2732.
- [63] L. J. Lawlor, K. Vasudevan, F. Grein, *J. Am. Chem. Soc.* **1978**, 100, 8062.
- [64] T. J. Lee, *J. Chem. Phys.* **1993**, 99, 9783.
- [65] T. S. Dibble, J. S. Francisco, *J. Chem. Phys.* **1994**, 100, 459.
- [66] M. E. Pendlum, S. Aloisio, J. S. Francisco, *Chem. Phys. Lett.* **1998**, 285, 164.
- [67] F. Angelelli, M. Aschi, F. Cacace, F. Pepi, G. de Petris, *J. Phys. Chem.* **1995**, 99, 6551.
- [68] E. L. Øiestad, E. Uggerud, *Int. J. Mass Spectrom.* **1999**, 185/186/187, 231.
- [69] J. I. Brauman, C. A. Lieder, M. J. White, *J. Am. Chem. Soc.* **1973**, 95, 927; W. E. Farneth, J. I. Brauman, *J. Am. Chem. Soc.* **1976**, 98, 7891; W. N. Olmstead, J. I. Brauman, *J. Am. Chem. Soc.* **1977**, 99, 4219; O. I. Asubiojo, J. I. Brauman, *J. Am. Chem. Soc.* **1979**, 101, 3715.

Received February 9, 2004